Pergamon

Journal of Structural Geology, Vol. 17, No. 7, pp. 1011 to 1024, 1995

0191-8141/95 $9.50+0.00

0191-8141(94)00116-2

Damage zone geometry around fault tips

ANNETTE G. McGRATH

Department of Geology, University of Leicester, Leicester, LE1 7RH, U.K.

and

IAN DAVISON*

Department of Geology, Royal Holloway, University of London, Egham, Surrey, TW20 OEX, U.K.

(*Received* 28 *March* 1994; *accepted in revised form* 20 *October* 1994)

Abstract—Damage zones are described around small scale normal, strike-slip, and reverse faults cutting horizontally-bedded carbonates, shales and siltstones in the Bristol Channel basin, U.K. Two different types of brittle damage zone have been recognized: (a) fractures branching directly from the fault tip; and (b) fractures forming an en échelon array, which are disconnected from the fault tip. Similar damage zones are repeated at regular intervals along the faults and they are interpreted to represent paleo-tip lines or sticking points along fault planes. Between these zones there is little visible damage outside the fault planes, which are typically 25–1000 μm thick along small displacement (<0.1 m) normal faults. Hence, faults propagated within their own plane at the scale of observation (25 μm), but dilational out-of-plane fractures are preserved at their arrested tips. Strike-slip and thrust faults were observed to produce more variable damage zone geometries compared to those at normal fault tips. Damage zone geometries around lateral tips of normal and strike-slip faults indicate that they can form by a different mechanism than up- and down-dip tip zones. Subsidiary fracture patterns can be used to recognize the direction of fault propagation.

INTRODUCTION

Damage zone geometry around faults can provide information on how faults propagate and are arrested. The growth of faults in rocks has been studied in laboratory experiments where tensile fractures are developed in the damage zone ahead of a propagating tip. Linkage of initial microcracks leads to a through-going fault plane (e.g. Cox & Scholz 1988, Petit & Barquins 1988). Crack development associated with fault growth has been extensively studied in theory (e.g. Lajtai 1974, Dey & Wong 1981, Segall & Pollard 1983) and small-scale deformation experiments (e.g. Brace & Bombolakis 1963, Friedman & Logan 1970, Tchalenko 1970, Kranz 1979, Gamond 1983, Horii & Nemat-Nasser 1986, Cox & Scholz 1988, Petit & Barquins 1988). These studies have shown that the induced faults do not propagate within their own plane, but that they initiate with en échelon fractures developed oblique to the growing fault. En échelon cracks permit higher stress concentrations to build-up in the bridge zones than would occur around isolated cracks (Bombolakis 1968), thus facilitating through-going fractures which link the isolated cracks. It is thought that the linking fractures between the en échelon tension cracks produce an irregular continuous crack surface which undergoes shear to produce a fault plane (e.g. Gamond 1983, Cox & Scholz 1988). The geometry of the linking fractures will depend on the geometry of the overlapping en échelon cracks, material properties and local heterogeneities at the grain scale.

Despite the large amount of theoretical and experimental work on fault and crack growth, there is relatively little published work on the geometry of naturally-induced brittle damage zone geometry around fault tips in rocks. Accurate analysis of damage zones would determine whether experimental and theoretical rock deformation studies are applicable to natural fault propagation in rocks. Most field observation has been focused on lateral (Rispoli 1981, Segall & Pollard 1983, Granier 1985, Martel *et al.* 1988) and up-dip (Einarsson & Eiríkson 1981, Jackson *et al.* 1992) tips of strike-slip faults. The study area provides a rare opportunity to examine and compare normal, reverse and strike-slip fault tips and their damage zones in the same rock types.

This paper describes the geometry of natural damage zones around meso-scale faults cutting layered sedimentary rocks. Crack-seal veins developed in pull-aparts along the fault zones and indicate that calcite and gypsum mineralization accompanied faulting after each individual slip event (Davison in press), so that fine-scale (<1 mm displacement) fracture damage is visible.

The difference in the extent of lithification and burial depth of the rocks during the extensional period in the early Jurassic and the inversion period during mid-Cretaceous to early Tertiary times is not accurately known. The fault and vein textures and temperatures of fault-related mineralization inferred from stable isotope data suggest that the extensional and contractional faults formed at a similar level of approximately 1 ± 0.5 km

*Author to whom all correspondence should be addressed.

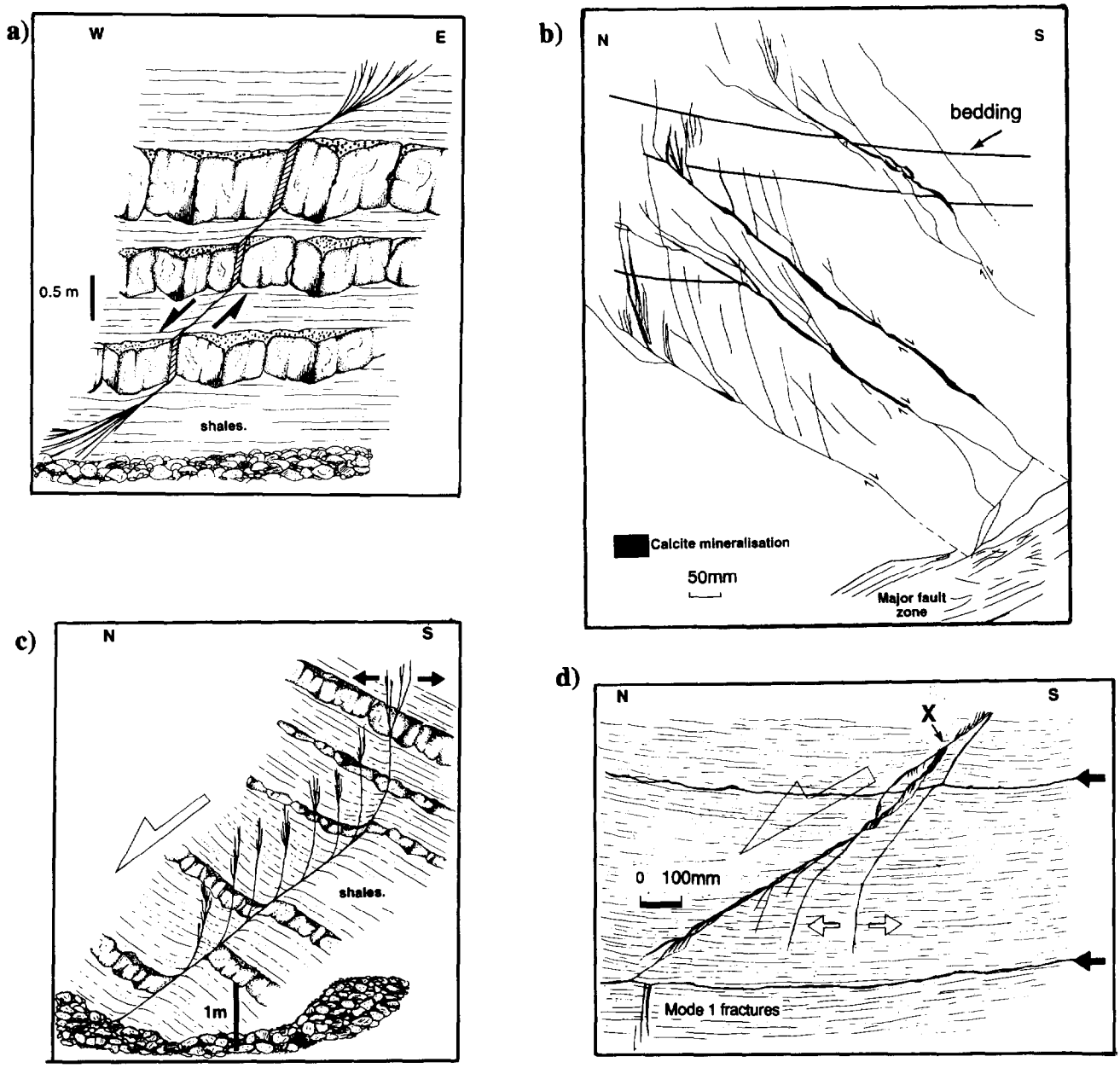

Fig. 1. (a) Sketch of a small normal fault at David's Way (ST 1290 4390), showing horsetail splays of fractures in the hangingwall of the fault at the upper and lower tips. The thicker slightly stippled beds are impure limestone. (b) Line drawing from a photograph showing a vertical cross-section through small normal faults at Kilve Beach (ST 1466 4448). The rocks are shales with several 1–5 cm thick layers of impure limestone. There are no fracture splays into the footwall of the faults, suggesting that they propagated upwards. (c) Sketch of a small normal fault below the Quadrant Range Hut between Kilve and Lilstock (ST 1608 4537). Thicker stippled beds are impure limestone. (d) Line drawing from a photograph showing the down-dip tip of a normal fault. X marks the location where the horsetail splays indicate that the fault propagated downwards, and above this the fault is interpreted to have propagated upwards. Arrows indicate small bedding-plane slip. Location below the pill box at Kilve (ST 1487 4460).

depth of burial (Hayward 1991, Davison in press). Besides brittle faulting there is evidence for plastic deformation of the shales, as folds are clearly developed along most normal faults without any discernible fracturing (e.g. Fig. 1a). These folds developed due to frictional drag across the fault plane accompanied by a component of fault propagation folding. However, it is not possible to ascertain the individual contributions of these two effects.

All the data presented are two-dimensional analyses in vertical section or horizontal map view. Mode 1 (opening), II (sliding) and III (tear) fracture nomenclature is used in this paper, where up- and down-dip tips of dip-slip faults and lateral tips of strike-slip faults are referred to as Mode II, and lateral tips of dip-slip faults and up- and down-dip tips of strike-slip faults are Mode III (Lawn & Wilshaw 1975). This terminology is usually used for cracks with little displacement, but is employed here to clarify the sense of shear. A fault tip point is defined as the point on the fault plane where visible simple shear displacement is zero.

REGIONAL GEOLOGY OF THE STUDY AREA

The study area is located on the southern edge of the Bristol Channel basin which formed in Triassic–Jurassic

times with the accumulation of up to 3.5 km of sediments in the centre of the basin, followed by a thin (<500 m) post-rift fill of Cretaceous–Tertiary age sediments (Kamerling 1979). There is no clear evidence of the depth at which normal faulting took place in Late Triassic–early Jurassic sedimentary rocks now exposed in coastal cliffs between Watchet and Lilstock. It was probably in excess of several hundreds of metres in order for sufficient compaction and lithification to have taken place, which allowed discrete fracturing and calcite mineralization during faulting. The basin was inverted during Cretaceous and Tertiary times with the formation of reverse and strike-slip faults. Vitrinite reflectance data from rocks in the study area suggest that inversion and subsequent erosion of at least 1.5 km, and possibly as much as 3 km, has occurred (Cornford 1986).

The faults examined between Quantoxhead and Lilstock cut Early Jurassic limestones and shales, with the shales making up to 75% of the sequence (Whittaker & Green 1983). The grey shales are calcareous and contain up to 28% total organic carbon (Cornford 1986). The limestones are well-cemented, and they are generally laterally persistent (>200 m), but some beds are lenticular or nodular and are probably produced by secondary diagenetic calcite precipitation. The individual limestone beds vary from approximately 0.1–0.75 m in thickness.

The faults in the shales and limestones were cemented with ferroan calcite soon after each fault slip event, evidenced by multiple crack-seal textures (Ramsay 1980) developed in pull-apart zones. Stable isotope studies on several of the normal faults indicate there is a disequilibrium between the wall rocks and the fluids which precipitated the ferroan–calcite fill, suggesting that the fluids came from a warmer (by 20–30°C) and presumably deeper (~1 km) source than the diagenetic fluids in the limestones (Hayward 1991, Davison in press). The stable isotopes from the inverted normal faults indicate temperatures of mineralization that are 10–15°C lower than extensional faults (Hayward 1991).

Faults in the Watchet area cut upper Triassic fine-grained reddish marls with occasional calcareous siltstones. The sediments are relatively homogeneous, and bedding is outlined by nodular gypsum concentrations or green diagenetic bands. The faults are cemented by locally-derived gypsum, and associated extensional fractures are often filled with fibrous gypsum which indicates the crack opening direction. For further information on faults and veins in this area see Peacock (1990, 1991) and Peacock & Sanderson (1991, 1992, 1994).

GEOMETRY OF FAULT DAMAGE ZONES

Normal faults

The general pattern of deformation associated with normal faults in the Early Jurassic shales and limestones consists of 45–75° dipping, E–W-striking faults which steepen to near vertical when they pass through the limestone layers (Fig. 1). Evidence from calcite-filled pull-aparts indicates that the dip of the normal faults changes during the initial formation of the normal faults. Extension in the limestones is produced by sub-vertical tensile fractures, and by normal faults in the shales; which link together to produce an irregular initial fault profile. Refraction is probably due to high pore pressure and lower strength in the shales (Peacock & Sanderson 1991, Sibson 1994). The fault profile is subsequently smoothed during later fault displacements. Calcite-filled fractures branch off the main fault plane at regular intervals (Fig. 1). In cross-sections perpendicular to the main fault plane, fractures splay from the main fault at an angle of approximately 20° then curve to a sub-vertical orientation away from the main fault zone. The vertical segments of the fractures are Mode I, as there is no vertical offset of the bedding (Figs. 1a & b). The fractures often bifurcate at their vertical tips into several individual strands (Fig. 1b). Spacing between the fracture splays varies between 30 and 200 mm in Fig. 1(b), where the faults have a maximum of 40–50 mm of displacement. Spacing is constant around 500 mm in Fig. 1c, where the fault has 750 mm of displacement. The fracture length at each splay zone appears constant along the fault profiles shown (0.2 m in Fig. 1b and 1.5 m in Fig. 1(c)). Examination of thin sections through normal faults between fracture splays indicate that the faults grow as very discrete planar fractures with finite widths of less than 25 μm (Fig. 2).

Lateral tips (Mode III edge) of normal faults can be observed in horizontal sections exposed on the foreshore (Fig. 3). In these cases the tips are characterized by fractures which continue along the same strike as the fault, before changing into an en échelon array of extensional fractures oriented about 10° oblique to the main fault plane (Fig. 3a). The oblique fractures are generally shorter and have a greater opening displacement near the fault tip compared to the most distal fractures (Fig. 3a). The fractured damage zone widens away from the fault tip and the individual fractures become more widely-spaced and slightly more oblique (20°) to the main fault. Small extensional faults (displacement <0.1 m) occasionally have single fractures which extend from the fault tip with the same strike as the main fault in map view. These tips are only observed in limestones and are due to the faults initiating in the limestones as Mode I fractures (see Peacock & Sanderson 1992). Hence, the lateral tips of normal faults can have different fracture geometries in the limestones, where a simple Mode I crack is developed, compared to that in the shales where oblique fractures would be developed at the Mode III fault edge.

The trace length of the splay fractures measured at lateral tips of normal faults on sub-horizontal limestone bedding planes appears to be positively related to maximum fault displacement (Fig. 4). The length over which fractures propagate beyond fault tips varies greatly for faults with similar maximum displacements, and can reach up to 45% of the total fault trace length at both lateral and down-dip tips (Fig. 1). Very different frac-

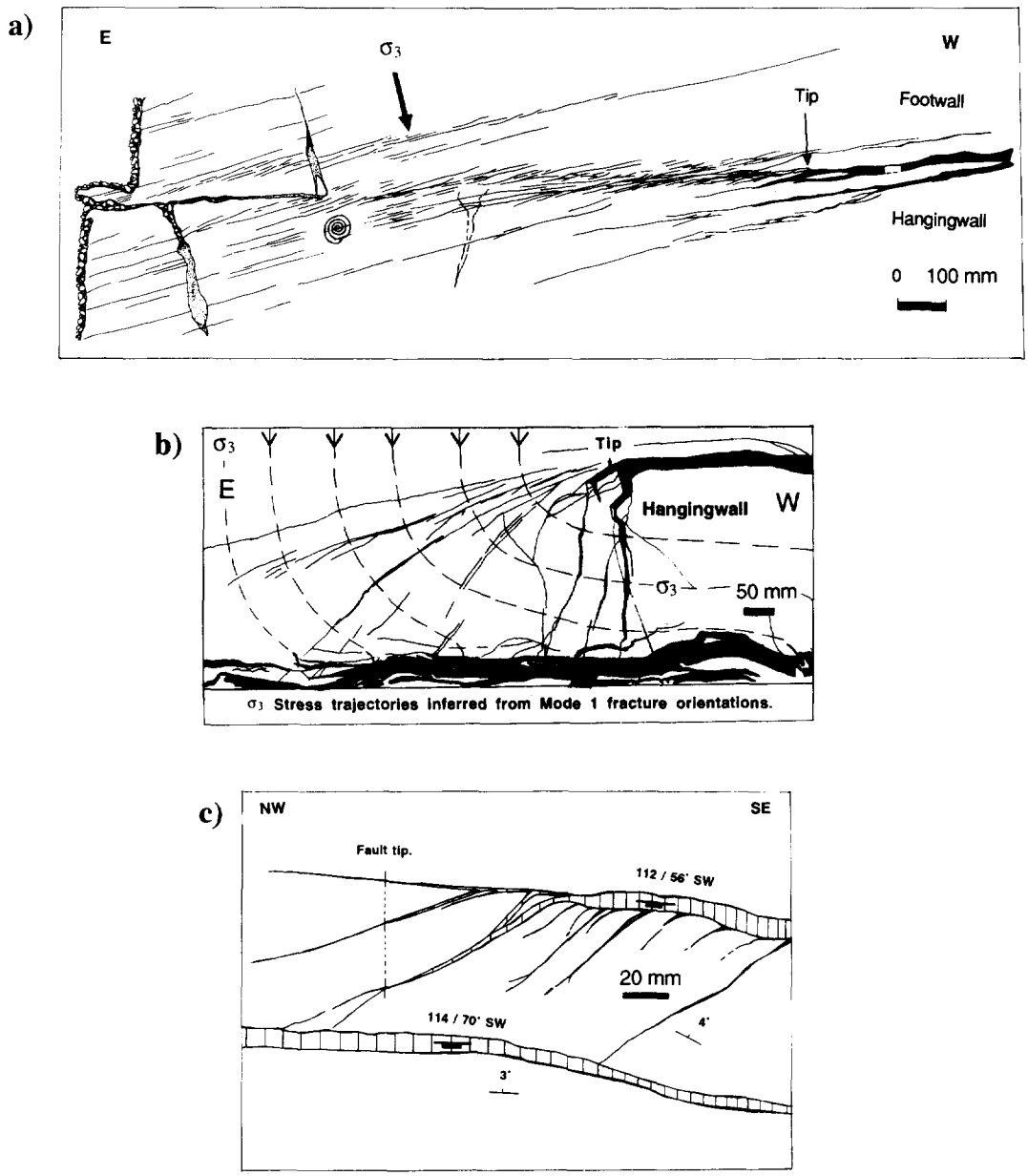

Fig. 3. (a) Plan view of the lateral termination of a normal fault on the Kilve foreshore (ST 1515 4464). It cuts through a horizontal limestone bed which exhibits fracture patterns with a calcite infill. The dotted areas to the left of the ammonite are weathered joints. (b) Line drawing of a photograph of a fault zone termination, where there is an adjacent fault (ST 1465 4448). (c) Line drawing of a photograph showing oblique fractures (mixed-mode) developed near a fault tip in a relay zone between two overlapping faults (ST 1349 4425).

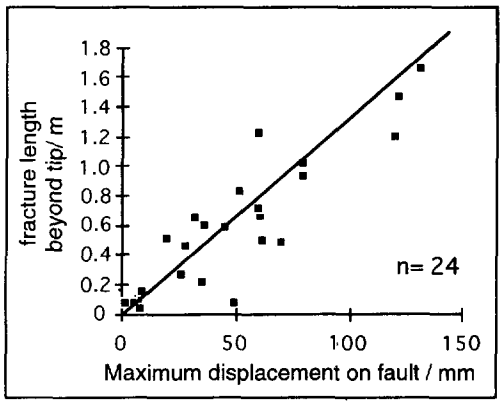

Fig. 4. Length of fractures in the damage zone in front of lateral fault tips (Mode III) plotted against the maximum displacement observed on normal fault traces. All measurements were taken in Early Jurassic limestones.

ture lengths can occur at the two lateral tips of the same fault. For example, fractures with lengths of 60 mm and 1600 mm were recorded beyond the opposite lateral tips of a normal fault with a maximum observed displacement of 520 mm. The maximum extent of fractures measured was 5.4 m, ahead of a fault tip where the maximum displacement on the fault reached 750 mm. The width of the calcite-filled fractures reaches a maximum of 12 mm at the fault tip and gradually tapers to zero. Unfortunately, it was not possible to observe the complete three-dimensional shape of the fractures at lateral tips. From two-dimensional observations it is inferred that they curve away from the fault tip, from an orientation parallel to the fault plane until the fractures are parallel to the maximum principal stress (σ_1) which was probably approximately vertical at the time of faulting (Fig. 1).

Fig. 2. Negative photomicrograph of small normal faults cutting through Early Jurassic limestones. Dark areas are Fe-rich calcite dilation zones along the faults. Where faults dip less steeply (~50°) no dilation is observed and the adjoining wall rocks do not exhibit any visible damage, suggesting that in-plane fault propagation has occurred. (Location ST 0460 4370).

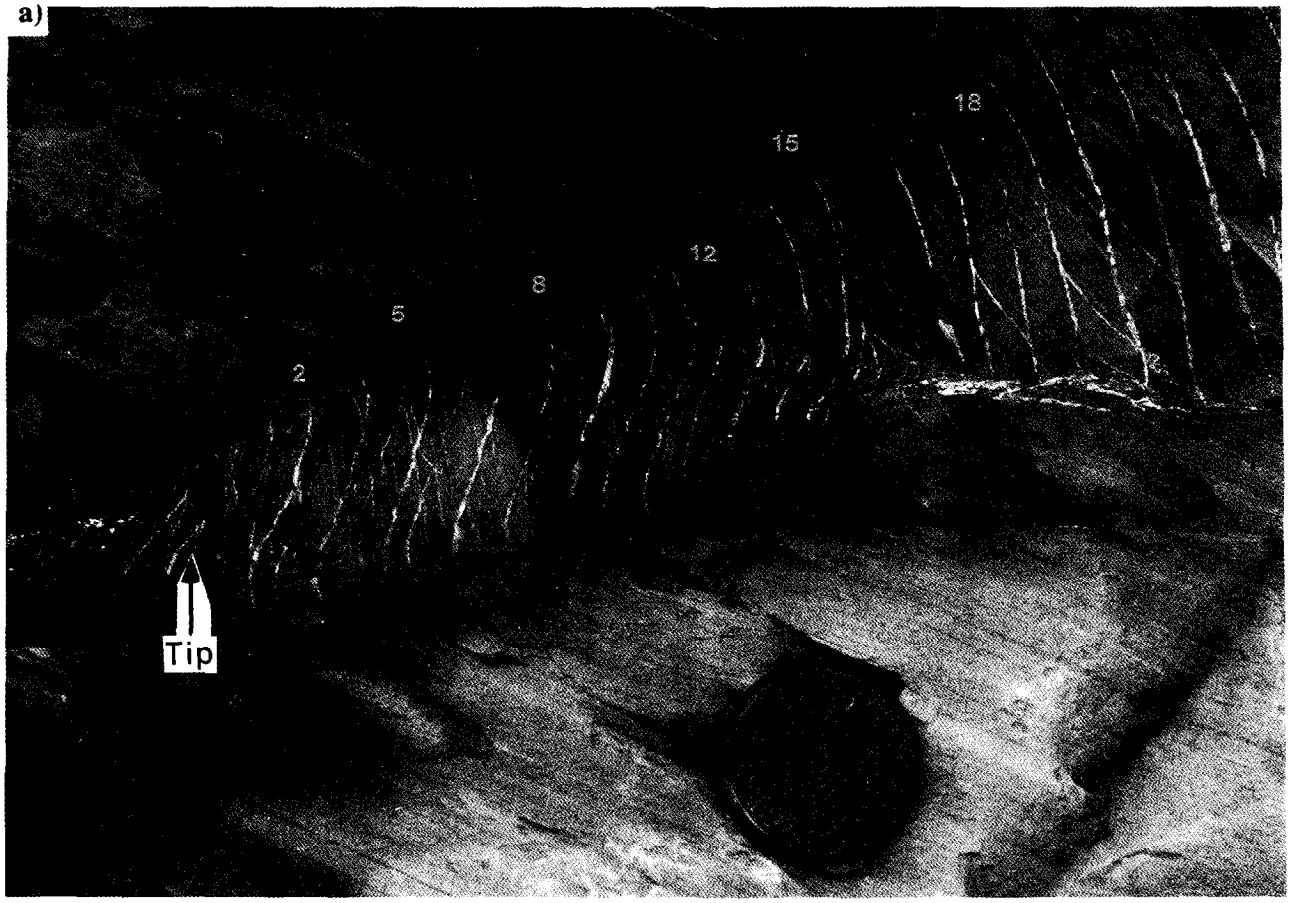

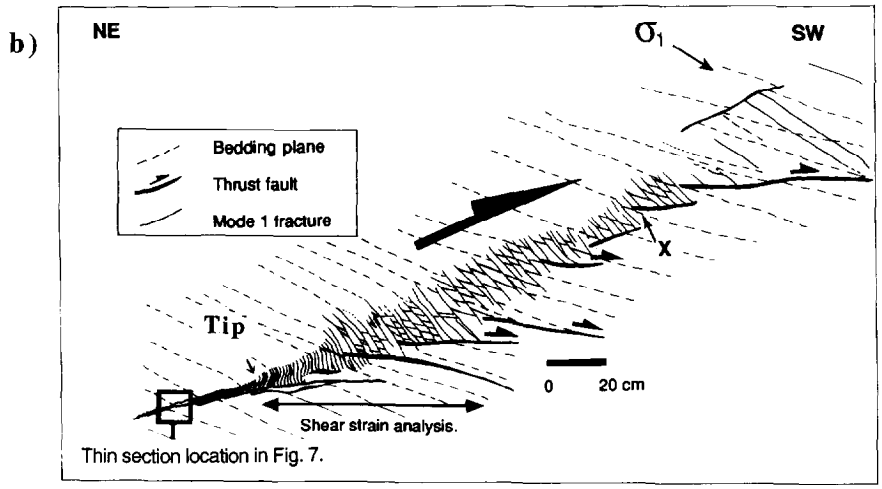

Fig. 5. (a) Photograph of a thrust termination at ST 1480 4448, showing a complex series of en échelon fractures and thrust faults formed in the thrust tip damage zone. Numbers refer to the shears measured in Fig. 6(d). (b) Line drawing of the thrust fault termination shown in (a). X marks the end of the zone where fractures have been rotated subsequently.

Where faults are overlapping in map view, oblique-slip faults curve sharply away from the main fault tip towards the adjacent fault and terminate in extensional fractures (Fig. 3b). This produces high displacement gradients at fault tips, and indicates that the principal stress orientations are markedly different at tips where interference between two faults occurred (compare Fig. 3a with Figs. 3b & c, see also Peacock & Sanderson 1991, 1994).

Thrust faults

The fault shown in Fig. 5 has a maximum observed displacement of 85 mm, and the damage zone ahead of the thrust fault tip extends for 2 m beyond the tip. The tip deformation zone is defined by calcite-filled faults and fractures, and broadens in an irregular way from the tip, from 40 mm to 450 mm in width. The strain in the tip zone produced the five deformation features described below (Fig. 5a).

(1) En échelon fractures are developed at approximately 45° to the main fault plane.

(2) A second generation of extensional fractures formed near to the fault tip parallel to the rotated bedding. Their extent is limited by the en échelon fractures as they do not appear to be cross-cut by them.

(3) Pervasive simple shear produced folding near the thrust tip, with accompanying clockwise rotation of the en échelon fractures and bedding.

(4) Reactivated original extensional fractures underwent shearing with reverse movement and have a maximum displacement of 8 mm.

(5) En échelon isolated synthetic thrust planes developed at regular intervals, oriented at approximately 20° to the main thrust fault. These limit the base of the damage zone and appear to have formed either before the en échelon fractures, which terminate against them near to the fault tip, or after them farther from the tip (Figs. 5a & b).

Fractures farthest away from the tip are straight and do not show any signs of shear parallel to their margins beyond point X in Fig. 5(b) and are more widely spaced than the fractures nearer the fault tip (Fig. 6a). The increase of the damage zone width, and the rapid decrease in the shear strain intensity (Fig. 6b) away from the tip indicates that the finite strain distribution is similar to the theoretical predictions of elevated stress distribution around isolated faults (e.g. Das & Scholz 1982). Pervasive shear strain (γ) in the centre of the damage zone reaches a maximum of 2.15 near the fault tip and decreases rapidly to 0.5 within a distance of 350 mm (Fig. 6d).

Shear strain across the damage zone has been calculated assuming that the earliest fractures formed at 45° to the shear zone, as they do in the most distal part. The central parts of the fractures have been subsequently rotated in a clockwise sense by simple shear whilst still propagating at approximately 45° to the fault plane at their tips (Ramsay & Huber, 1987, Fig. 6b). Traverses across the shear zone at every fourth fracture indicate that the shear strain decreases away from the fault tip and is reduced dramatically where secondary synthetic thrust faults occur (Fig. 6d).

Thin sections from the main fault zone show that it is composed of alternating slivers of wall rock and sheared and folded calcite veins (Fig. 7). This progressive shearing of the original fractures makes it difficult to observe initial geometries of the damage zone where the fault appears to have propagated within its own plane at the scale of observation (1–3 mm).

Simple thrust tips with horsetail fractures are also present (Fig. 8). In this example, the fractures curve very abruptly away from the fault towards the inferred remote principal stress direction, which lies at a high angle (75°) to the fault plane (Fig. 8). The fractures have a length approximately equal to the maximum displacement on the fault (40 mm).

In summary, up-dip Mode II thrust tip zones can be more complex than extensional Mode II fault tip zones, and larger more intense damage zones are produced. However, simple horsetail fractures, similar to normal tips, are also observed.

Strike-slip faults

Strike-slip faults are seen to terminate up and down dip (Mode III) and laterally (Mode II), with fractures splaying off the main fault. The fractures branch off at intervals along the fault and at fault tips. In plan view, they are inclined at angles which vary between 25° and 80° to the main fault (Fig. 9). Fibrous calcite has grown in these fractures and the fibres are oriented at 90° to the fracture walls, indicating that they are purely Mode I fractures at their tips. These fractures can branch off the main fault as straight features at an angle greater than 45° (Fig. 9a), or curve slightly toward σ_1 (Fig. 9b). They are wedge-shaped with the greatest amount of opening at the contact with the main fault (Fig. 9a). This enables large fault-parallel displacement gradients to develop at the tip. These offshoot fractures are probably abandoned when the fault shears through them. The strike-slip faults exhibit prominent pull-apart zones which are interpreted to mark the position where two faults linked together across a dilational jog. The irregular displacements, measured by the width of pull-aparts, along these faults support the hypothesis that they are formed by connection of individual strands (e.g. Fig. 9d, Ellis & Dunlap 1988). The strike-slip faults are interpreted to have followed pre-existing joints, evidence for this is that such faults are not observed in areas where east–west joint sets are absent. The regional compression direction during strike-slip faulting was oriented approximately north–south, at a high angle to these faults and thus required an initially weak plane or high pore fluid pressure to allow fault movement. Very similar strike-slip faults have been described along reactivated joints in granites from the Sierra Nevada (Segall & Pollard 1983).

Another pattern of strike-slip fault termination involves continuous bifurcation of the strike-slip faults,

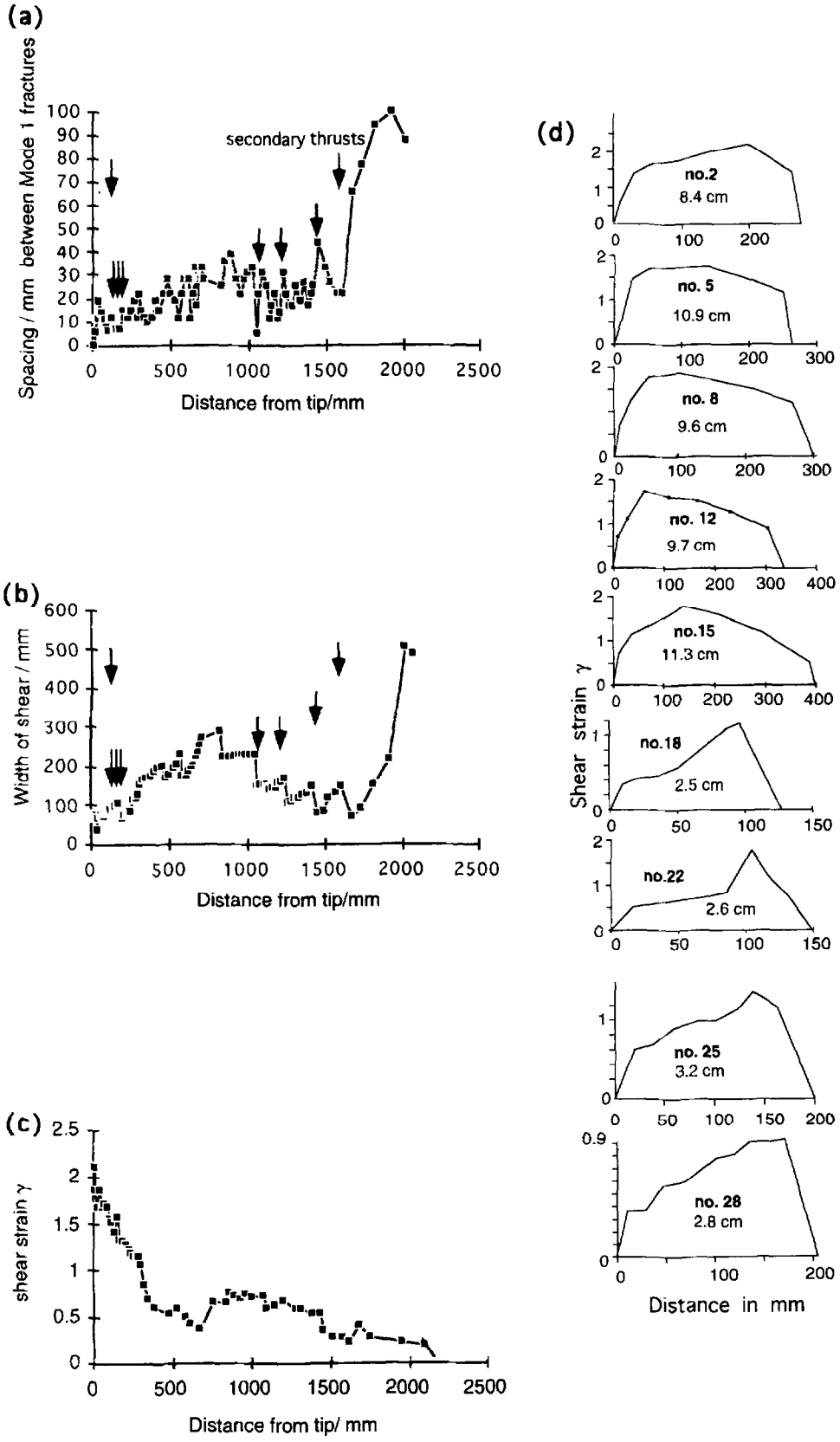

Fig. 6. Analysis of the damage zone shown in Fig. 5.(a) Plot of spacing of the en échelon fractures against distance along the damage zone measured from the fault tip. (b) Plot of width of the shear zone defined by fracture length measured perpendicular to the main fault plane. (c) Plot of maximum shear strain at the centre of the damage zone against distance from the fault tip. (d) Plots of shear strain across the damage zone at regular intervals along the damage zone. Numbers under the curves are shear displacements calculated in centimetres across the damage zone using the observed rotation of the fractures which are assumed to have formed at 45° to the shear zone.

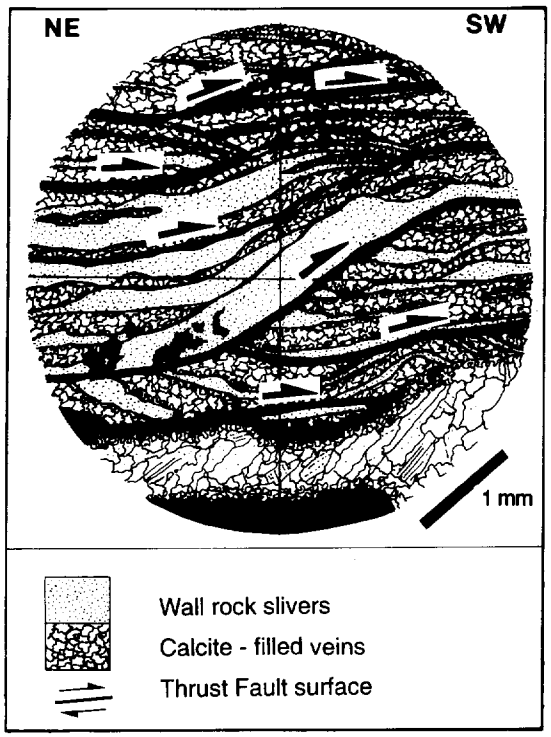

Fig. 7. Line drawing of a thin section through the thrust fault zone. Location of the thin section is shown on Fig. 5(a). Thin screens of wall rock are separated by calcite-filled veins which were extension fractures oriented oblique to the fault. These have been rotated and sheared through by later thrusting. Black areas are holes in the section.

with many fracture splays formed at the tips of the smaller faults (Fig. 9c). The subsidiary synthetic strike-slip faults are regularly oriented at approximately 20° to the main fault, and the extensional fracture splays are oriented at approximately 45° to the subsidiary strike-slip faults (Fig. 9c). The example shown here splits from a single fault strand to over 30 separate strands in a horizontal distance of 1 m.

The up-dip tips of the strike-slip faults are rarely seen, but when observed exhibit a series of bifurcating fractures, which terminate in the vertical plane parallel to σ_1 (Fig. 10). These are interpreted to be Reidel shears which splay off from the main fault and have a helicoidal geometry (e.g. Naylor *et al.* 1986).

Lateral tips of strike-slip faults have been observed where there is a change in strike at the end of the fault (Fig. 11a). They exhibit a damage zone which widens away from the fault (Fig. 11a). Displacement is transferred from the main fault onto antithetic shears and Mode I fractures. The Mode I fractures open up at approximately 45° to the main sinistral fault plane (Fig. 11a). Anticlockwise rotation of these fractures occurred in this example, so that they were reactivated and underwent later antithetic dextral shear. Further fracturing occurred at the tips of the antithetic shears, with the most prominent Mode I fractures splaying from the shears nearest to the fault tip (Fig. 11a). This reactivation causes triangular wedges to pull-apart at the tips of the antithetic shears (Fig. 11a). These en échelon faults separate what is effectively a series of rotating and bending domino blocks (Fig. 11b). The main fault sheared through the base of the dominoes, with calcite-filled dilational zones developed along the contact between the dominoes and the main fault (Fig 11b). The secondary shears have an antithetic shear sense in both cases (Figs. 11a & b).

Strike-slip faults appear to produce the greatest observed variation of damage zone geometries. The reason for this is probably that we have observed strike-slip fault tips arrested in transpressional, transtensional and simple shear stress regimes.

DISCUSSION

It is still highly debatable whether true Mode II and III in-plane fracturing occurs in natural rocks, as it has never been observed in experimental deformation (e.g. Petit & Barquins 1988). However, Lawn & Wilshaw (1975) suggest this may be possible where large confining stresses suppress Mode I fracturing, and Lin & Parmentier (1988) also suggest that in-plane Mode II and III fault propagation can occur with high confining stresses and low rock plasticity. The splays of horsetail fractures branch off the main fault at regular intervals. In between fracture splays there is little or no fault damage visible except within the fault zone, which may be as narrow as 25 μm (Fig. 2). Thin sections examined

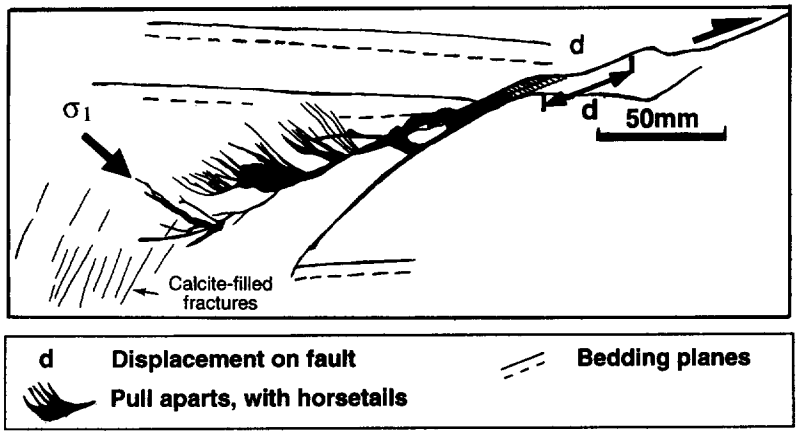

Fig. 8. Down-dip thrust fault tip with closely-spaced fractures splaying from the main fault, and with calcite filled pull-aparts along the main fault plane (ST 1823 1541, east of Lilstock).

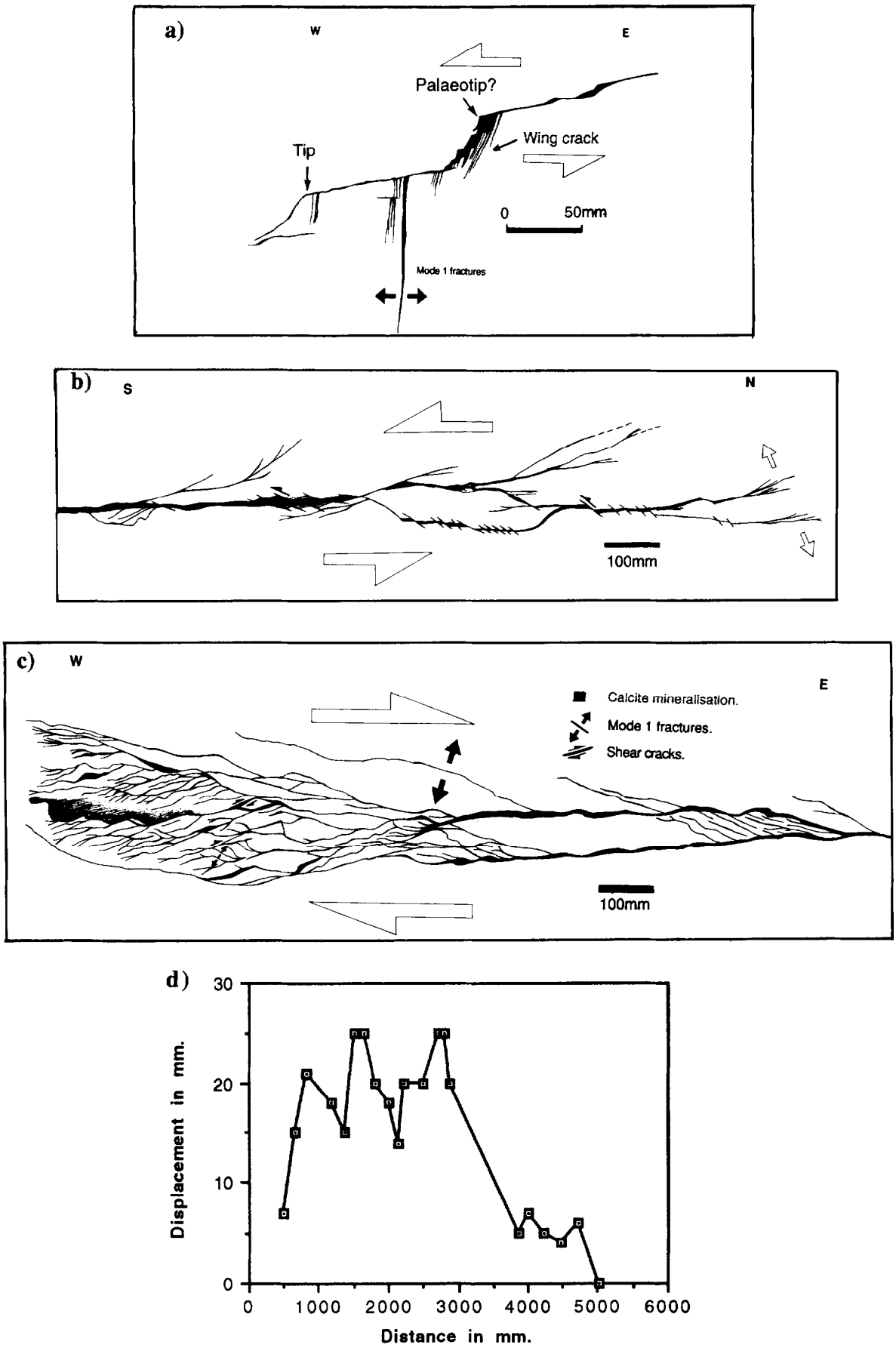

Fig. 9. (a) Strike-slip fault termination exposed on a sub-horizontal bedding plane in limestones. The fractures splay from the fault tip and pull-apart parallel to the maximum principal stress direction (σ_1) (ST 1360 4424). (b) Strike-slip fault tip in Early Jurassic limestones, with a splay of fractures which gently curve towards the σ_1 direction (ST 1360 4424). (c) Strike-slip fault tip in Triassic red marly siltstones characterized by bifurcation of a principal fault into many smaller strands (ST 0783 4350). (d) Displacement-distance relationship along a strike-slip fault cutting Triassic marl approximately 500 m west of Watchet harbour (ST 0780 4340).

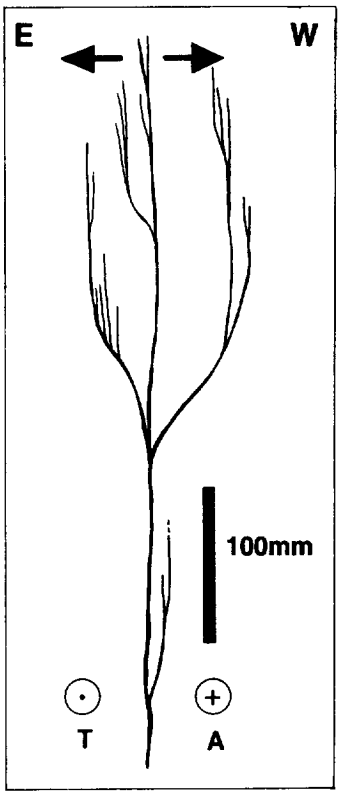

Fig. 10. Up-dip termination of a vertical section through a strike-slip fault, showing a splay of fractures which branch off the main fault at angles of 20–40° and curve towards the vertical (ST 1360 4424).

along the main fault plane in between damage zones in the shales and limestones indicate that dilation zones are present along most of the main fault zone. Small out-of plane Mode I fractures may have been produced ahead of the propagating fault tip to produce a finite width of the fault zone (<25 μm for faults with less than 10 mm displacement). These observations indicate that in-plane fault propagation occurred at the scale of thin section observation (25 μm) when dynamic rupturing at high differential stresses occurred, and when the faults were arrested at lower stresses they terminate with out-of plane fractures.

All three models of faulting exhibit Mode II edges with horsetail splays of mixed-mode fractures, which curve away from the fault towards the regional maximum principal stress orientation and terminate as Mode I fractures. Experimental work indicates that low differential and confining stresses are required to initiate crack branching and horsetail formation (Petit & Barquins 1988, Wawersik & Brace 1971). Yoffe (1951) has suggested that for Mode I fracturing in isotropic materials crack-branching (out-of plane) can occur when the crack reaches its terminal propagation velocity. Latjai (1969) has investigated fault branching using mechanical theory, and explains crack branching occurring due to zero or low normal stress acting across planes oriented perpendicular to the fault slip direction (termed transverse normal stress). The angle that splay fractures make with the main fault mainly depends on the rock plasticity, stress conditions, and fault surface geometry (Lin & Parmentier 1988).

Experimental work on engineering materials with carefully designed rigs has inhibited out-of plane tensile fracturing so that Mode II and Mode III fractures grow and fracture toughness can be investigated (Chisholm & Jones 1977, Agarwal & Giare 1981, Banks-Sills *et al.* 1983, Davies, *et al.* 1985). Photoelastic experiments on epoxy resin indicate that Mode II fracture toughness (K_{IIc}) is greater than Mode I fracture toughness (K_{Ic}) (Chisholm & Jones 1977); and experimental deformation of randomly oriented glass-fibre composites has indicated that Mode III fracture toughness (K_{IIIc}) is greater than Mode II (Agarwal & Giare 1981). If this is the case in rocks ($K_{IIIc} > K_{IIc} > K_{Ic}$), it may explain why there is a difference in damage zone geometries at Mode II and III normal fault tips, with unlinked en échelon fractures forming ahead of Mode III fault tips due to the higher stresses required to propagate the fracture front.

Two basic types of damage zone have been recognized with several different types of fracture pattern (Fig. 12). The first group consist of fractures which are mainly connected to the main fault (wing and horsetail fractures). The simplest damage zone geometry was observed on lateral tips of small normal faults in the limestone beds (<500 mm displacement) where a single dilational calcite-filled fracture continues with the same strike as the main fault and progressively decreases in width away from the tip (Fig. 12a). Horsetail fractures are often present in the shales and they curve away and bifurcate from the fault tip. They are interpreted to propagate towards the direction of the maximum remote princpal stress (σ_1) (Brace & Bombolakis 1963, e.g. Figs. 1, 12b and 13).

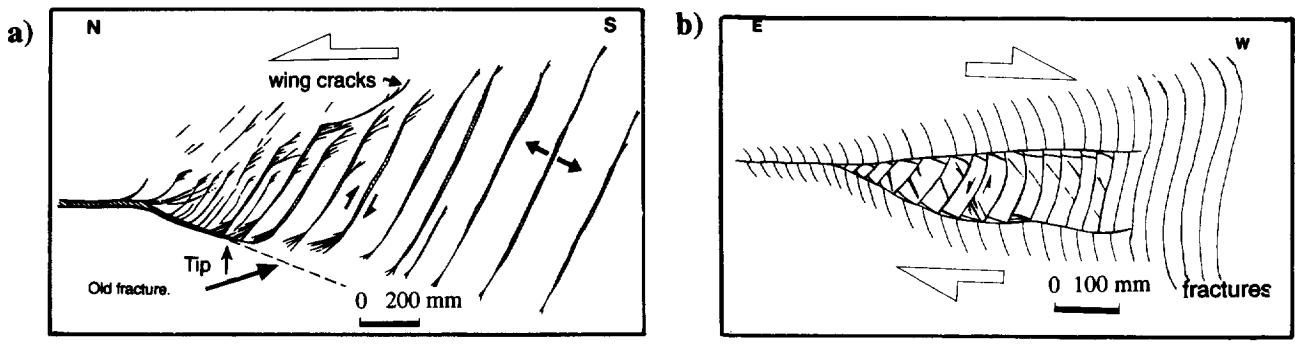

Fig. 11. Map views of strike-slip fault tips. (a) Transpressional fault tip showing a widening zone of en échelon fractures away from the fault tip (ST 0477 4366). (b) Dextral strike-slip fault with antithetic second-order shears at the tip formed between two branches of the propagating fault (ST 0780 4328).

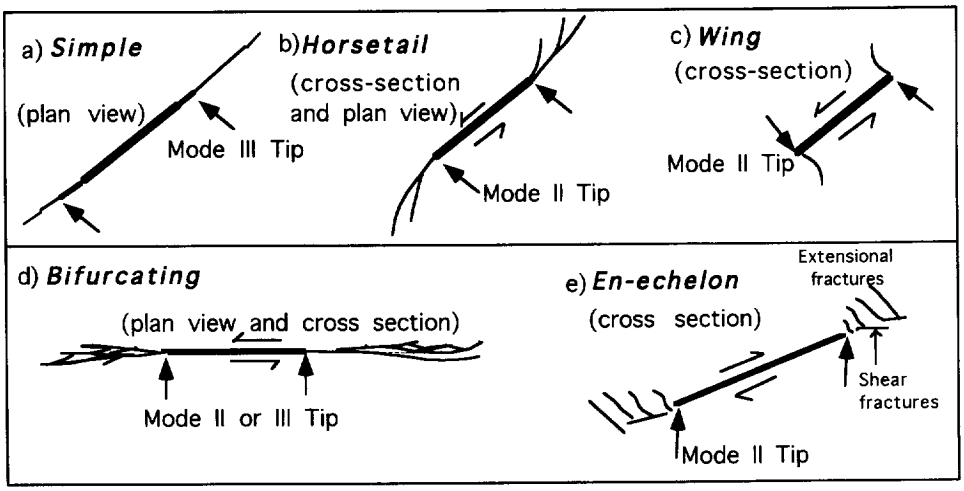

Fig. 12. Summary diagram of observed fracture patterns of fault tip damage zones. (a) Simple vertical fractures, which continue with the same strike as the main fault and progressively decrease in width away from the tip. These fractures are only observed at lateral tips of normal faults in limestones. (b) Horsetail fractures which curve away from the tip towards the maximum principal stress (σ_1). (c) Wing fractures curving towards the maximum principal stress direction (e.g. Fig. 9a). (d) Bifurcating patterns of fractures, produced by interaction of Riedel shears and extensional fractures, which were only observed along strike-slip faults (e.g. Fig. 9c). (e) En échelon fractures which increase their length and spacing progressively away from the fault. These are linked after rotation, due to new fractures formed in cross-cutting orientations almost parallel to the main fault plane.

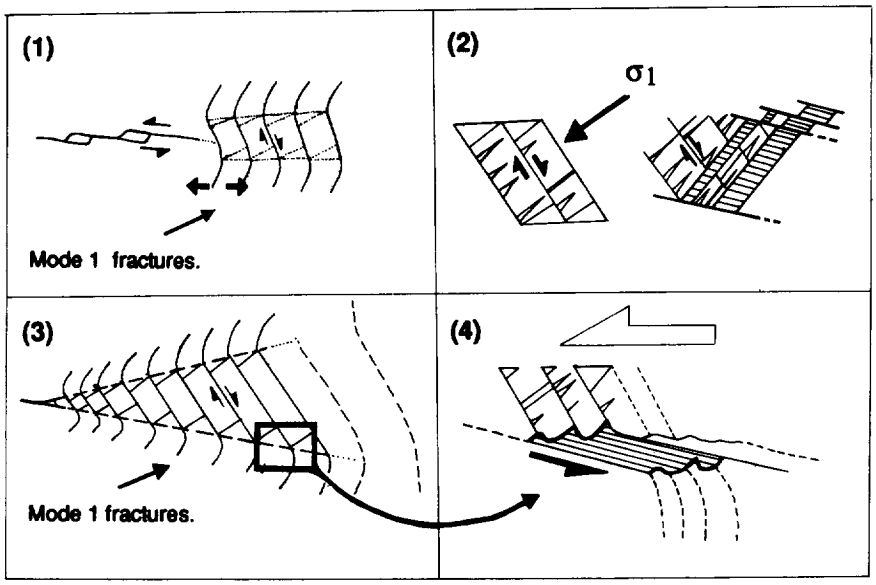

Fig. 13. Schematic sequence of events suggested for the evolution of a Mode II edge strike-slip damage zone. (1) Formation of fractures and subsequent rotation and activation as antithetic shears. (2) Locking of the antithetic shears and formation of Mode I fractures. (3) Deformation linked along the boundaries of the rotating blocks producing dilation in (4).

Horsetail fractures splaying from the faults may indicate either paleo-tip points, or sticking points along the fault. Horsetails can be used to track the propagation direction of the fault (Friedman & Logan 1970). For example, all the normal faults shown in Fig. 1(b) must have propagated upwards from a N-dipping fault below them, as all the fracture splays occur in the hangingwall. Fracture splays would be present in the footwall of these faults if the faults had propagated downwards. Similarly, the fault in Fig. 1(c) is interpreted to have propagated upwards, and the fault shown in Fig. 1(d) propagated downward from point X.

Wing fracture patterns were only observed associated with strike-slip faults. (e.g. Figs. 11a and 12c). Theoretical studies and laboratory experiments on glasses and ceramics (Brace & Bombolakis 1963, Latjai 1971, Shamina *et al.* 1975, Horii & Nemat-Nasser 1986, Pollard & Segall 1987, Petit & Barquins 1988) of Mode II fault edges indicate that wing fractures propagate from the fault tip at an angle of approximately 70° to the main fault and curve to be parallel with the remote maximum principal stress (Fig. 12c). Rispoli (1981) has also described a similar arrangement of wing fractures at Mode II tips of small strike-slip faults in limestones. This type of fracture is very rare in the study area, and was only observed on strike-slip Mode II fault edges. Experiments on glass indicate that formation of wing cracks occurs in uniaxial compressive tests, whereas horsetail

cracks are produced in biaxial compressive tests (Petit & Barquins 1988). Hence, tensional stresses are thought to induce wing-crack formation which may form in rocks under high pore pressure conditions, or low confining pressures.

The other basic type of damage zone consists of shear zones with en échelon dilational fracture systems, where individual fractures increase their length and spacing away from the fault tip (Figs. 4b and 12e). These progressively link after rotation, due to subsidiary fractures formed obliquely to the initial fractures (Fig. 9c). Shear zones similar to those described have been induced in glass at higher differential loading and confining pressures than those required to produce horsetails and wing cracks (Petit & Barquins 1988).

Mode II edges of normal faults were observed to produce damage zones with out-of plane horsetail fractures which link directly to the fault tip (Table 1). Mode III edges produced isolated en échelon fractures which are not directly linked to the tip (Table 1). These fractures form at an oblique angle up to 10° from the main fault plane, in plan view. This indicates that the stress regimes and resulting damage zone geometry are different at Mode II and Mode III edges of extensional faults. This may be due either to the different mode of fracture propagation or the difference in the orientation of the layering in relation to the direction of fault tip propagation. Strike-slip faults were observed to produce horsetail, bifurcating or en échelon patterns at lateral tips (Mode II), but only bifurcating patterns at up-dip (Mode III) tips (no down-dip strike-slip fault tips have been observed, Table 1). Thrust faults were observed to produce damage zones with either horsetail fractures or shear zones with en échelon fracture patterns (with up to 50° obliquity between fractures and the main fault plane observed in cross-sections). Lateral thrust tips were not observed.

King & Sammis (1992) have suggested a fault propagation mechanism where en échelon tension fractures separate slabs of rock which are bent due to shearing. They suggested this bending would produce a second series of extensional fractures oriented at right angles to the original set. Our observations of lateral tips of some strike-slip faults suggest that the en échelon fractures act in a similar way to domino faults and rotation causes locking of the faults once they are rotated and oriented almost orthogonally to the σ_1 direction. Subsidiary fractures propagate obliquely or perpendicularly to the first en échelon array according to the local orientation of σ_1 (Figs. 11 and 13).

Table 1. Summary of different types of damage zone fracture geometries observed at fault tips (shown in Fig. 12)

Type of fault	Up- and down-dip tips	Lateral tip
Normal fault	Horsetail	Simple, horsetail and en échelon
Strike-slip fault	Bifurcating	Wing, horsetail, bifurcating and en échelon
Thrust fault	Horsetail and en échelon	?

There is a general linear increase in average length of the extent of fractures which continue along strike beyond the Mode III lateral tips of normal faults with increasing maximum displacement of the fault (Fig. 4). This suggests that larger faults exert greater damage. Larger faults may be arrested by harder sticking points, resulting in greater precursor damage before the fault propagates further.

CONCLUSIONS

(1) All damage zones in the Watchet-Kilve area terminate in mixed mode or Mode I fractures. Mixed-mode horsetail fractures curve away from the main fault plane towards the remote maximum principal stress direction to terminate in Mode I cracks (Fig. 14).

(2) Several basic patterns of damage zone were repeatedly observed, which only occur in either one or two of the three basic fault types (Table 1). By comparison with experimental deformation tests, wing cracks are thought to be produced at low confining or tensile stresses. Horsetail fractures are probably produced at intermediate differential stresses and shear zones with dilatant en échelon fractures occur at the highest stresses.

(3) Thrust and strike-slip faults have more variable damage patterns than normal faults. This could be due to the higher variations in stress build-up at thrust and strike-slip fault tips, but could also be due to the different orientation of the layering in relation to the principal stresses in each of the three fault types. The control of layering on fault propagation in rocks has still not been investigated thoroughly in experimental or theoretical studies.

(4) Faults were observed to propagate within their own plane at the scale of thin section observation with damage zones less than 25 μm in thickness. Damage zones widen and only produce large out-of plane fractures when the fault is arrested or reaches a barrier.

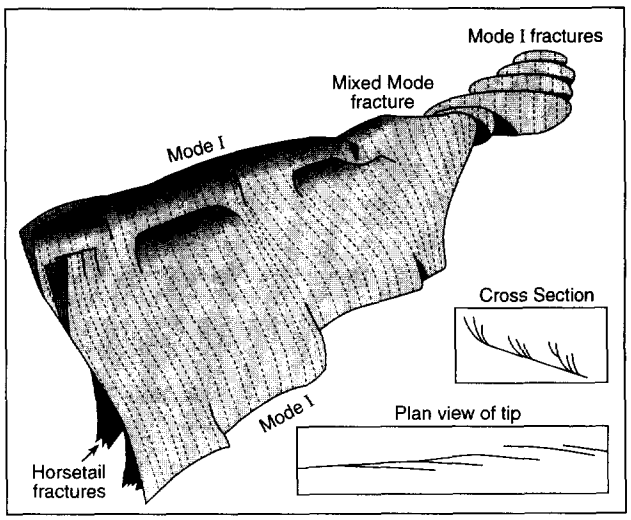

Fig. 14. Summary of the three dimensional geometry of fractures in damage zones around a normal fault which have horsetail splays at the Mode II edges and en échelon fractures at the Mode III edges.

(5) These observations highlight the apparent paradox that natural faults are planar features which appear to propagate within plane, although damage zones with out-of plane fracturing are consistently observed in rock deformation experiments and at arrested natural fault tips.

Acknowledgements—A. McGrath would like to thank the Natural Environment Research Council for supporting her one year post-graduate M.Sc. studentship on the Basin Evolution and Dynamics course held at Royal Holloway, University of London where this work was undertaken. We are grateful for very helpful reviews by Roland Bürgmann and David Peacock.

REFERENCES

Agarwall, B. D. & Giare, G. S. 1981. Fracture toughness of short fibre composites in Mode II and III. *Engng. Frac. Mech.* **15**, 219–239.

Atkinson, B. K. 1984. Sub-critical crack growth in geological materials. *J. geophys. Res.* **89**, 4077–4114.

Atkinson, B. K. (Ed.) 1987. *Fracture Mechanics of Rock*. Academic Press, London.

Banks-Sills, L., Arcan, M. & Bui, H. D. 1983. Toward a pure shear specimen for K_{II} determination. *Int. J. Fract.* **22**, R9–R14.

Bombolakis, E. G. 1968. Photoelastic study of initial stages of brittle fracture in compression. *Tectonophysics* **1**, 343–351.

Brace, W. F. & Bombolakis, E. G. 1963. A note on brittle crack growth in compression. *J. geophys. Res.* **68**, 3709–3713.

Chisholm, D. B. & Jones, D. L. 1977. An analytic and experimental stress analysis of a practical Mode II fracture test specimen. *Exper. Mech.* **17**, 7–13.

Cornford, C. 1986. The Bristol Channel Graben: organic geochemical limits on subsidence and speculation on the origin of inversion. *Proc. Ussher Soc.* **6**, 360–367.

Cox, S. J. D. & Scholz, C. H. 1988. On the formation and growth of faults. *J. Struct. Geol.* **10**, 413–430.

Das, S. & Scholtz, C. 1982. Off-fault aftershock clusters caused by shear stress increase? *Bull. seism. Soc. Am.* **71**, 1669–1675.

Davies, J. Morgan, T. J. & Yin, A. W. 1985. The finite element analysis of a pure-through shear specimen in mode II. *Int. J. Fract.* **28**, R3–R10.

Davison, I. 1995. Fault slip evolution determined from crack-seal veins in pull-aparts and their implications for general slip models. *J. Struct. Geol.* **17**, 1025–1034.

Dey, T. N. & Wang, C. Y. 1981. Some mechanisms of microcrack growth and interaction in compressive rock failure. *Int. J. Rock. Mech. Sci. & Geomech. Abstr.* **18**, 199–209.

Einarsson, P. & Eiríksson, J. 1981. Earthquake fractures in the Districts Land and Rangárvellir in the South Iceland Seismic Zone. *Jokull* **32**, 113–120.

Ellis, P. G. & Dunlap, W. J. 1988. Displacement variation along thrust faults: implications for development of large faults. *J. Struct. Geol.* **10**, 183–192.

Freidman, M. & Logan, J. M. 1970. Microscopic feather fractures. *Bull. geol. Soc. Am.* **81**, 3417–3420.

Gamond, J. F. 1983. Displacement features associated with fault zones: A comparison between observed examples and experimental models. *J. Struct. Geol.* **5**, 33–45.

Granier, T. 1985. Origin, damping and pattern of development of faults in granite. *Tectonics* **4**, 721–737.

Hayward, R. 1991. Mineralisation in Fault Zones, Watchet, N. Somerset. M.Sc. thesis, unpublished, Royal Holloway, University of London, London.

Horii, H. & Nemat-Nasser, S. 1986. Brittle failure in compression: splitting, faulting and brittle-ductile transition. *Phil. Trans. Roy. Soc. Lond.* **319**, 337–374.

Jackson, M. D., Endo, E. T., Delaney, P. T., Arnadottir, T. & Rubin, A. M. 1992. Ground ruptures of the 1974 and 1983 Kaoiki earthquakes, Mauna Loa volcano, Hawaii. *J. Geophys. Res.* **97**, 8775–8798.

Kamerling, P., 1979. The geology and hydrocarbon habitat of the Bristol Channel Basin. *J. Pet. Geol.* **2**, 75–93.

King, G. C. P. & Sammis, C. 1992. The mechanisms of finite brittle strain. *Pure & Appl. Geophys.* **138**, 611–640.

Kranz, R. L. 1979. Crack-crack and crack-pore interactions in stressed granite. *Int. J. Rock Mech. Min. Sci. Geomech. abs.* **16**, 37–47.

Lawn, B. R. & Wilshaw, T. R. 1975. *Fracture of Brittle Solids*. Cambridge University Press, Cambridge.

Lajtai, E. Z. 1969. Mechanics of second order faults and tension gashes. *Bull. geol. Soc. Am.* **80**, 2253–2272.

Lajtai, E. Z. 1971. Experimental evaluation of the Griffith theory of brittle failure. *Tectonophysics* **11**, 129–156.

Lajtai, E. Z. 1974. Brittle fracture in compression. *Int. J. Fract.* **10**, 525–536.

Lin, J. & Parmentier, E. M. 1988. Quasistatic propagation of a normal fault: a fracture mechanics model. *J. Struct. Geol.* **10**, 249–262.

Martel, S. J. & Pollard, D. D. 1989. Mechanics of slip and fracture along small faults and simple strike-slip fault zones in granitic rock. *J. geophys. Res.* **94**, 9417–9428.

Martel, S. J., Pollard, D. D. & Segall, P. 1988. Development of simple strike-slip fault zones in granitic rock. Mount Abbot quadrangle, Sierra Nevada, California. *Bull. geol. Soc. Am.* **99**, 1451–1465.

McGrath, A. 1992. *Fault Propagation and Growth, a Study of the Triassic and Jurassic from Watchet and Kilve, North Somerset*. M.Sc. thesis, unpublished, Royal Holloway, University of London, London.

Naylor, M., Mandl, G. & Sijpestein, C. H. K. 1986. Fault geometries in basement-induced wrench faulting under different initial stress states. *J. Struct. Geol.* **7**, 737–752.

Palmer, C. P. 1972. The lower Lias (lower Jurassic) between Watchet and Lilstock in north Somerset (U.K.). *Newsletter Stratigraphy* **2**, 1–30.

Peacock, D. C. P. 1990. Displacement and segment linkage in fault zones. Unpublished Ph.D. thesis, University of Southampton, Southampton.

Peacock, D. C. P. 1991. A comparison between the displacement geometries of veins and normal faults at Kilve, Somerset. *Proc. Ussher Soc.* **7**, 262–267.

Peacock, D. C. P. & Sanderson, D. J. 1991. Displacements, segment linkage and relay ramps in normal fault zones. *J. Struct. Geol.* **13**, 721–733.

Peacock, D. C. P. & Sanderson, D. J. 1992. Effects of layering and anisotropy on fault geometry. *J. Geol. Soc. Lond.* **149**, 793–802.

Peacock, D. C. P. & Sanderson, D. J. 1994. Geometry and development of relay ramps in normal fault systems. *Bull. Am. Ass. Petrol Geol.* **78**, 147–165.

Petit, J.-P. & Barquins, M. 1988. Can natural faults propagate under Mode II conditions? *Tectonics* **7**, 1243–1256.

Pollard, D. D. & Segall, P. 1987. Theoretical displacements and stresses near fractures in rocks: with applications to faults, joints, veins, dikes and solution surfaces. In: *Fracture Mechanics of Rock* (edited by Atkinson, B. K.). Academic Press Inc, London, 277–349.

Pollard, D. D., Segall, P. & Delaney, P. T. 1982. Formation and interpretation of dilatant echelon cracks. *Bull. geol. Soc. Am.* **93**, 1291–1303.

Price, N. J. 1966. *Fault and Joint Development in Brittle and Semi-brittle Rocks*. Pergamon Press, London.

Ramsay, J. G. 1980. The crack-seal mechanism in rocks. *Nature* **284**, 135–139.

Ramsay, J. G. & Huber, M. 1987. *The Techniques of Modern Structural Geology, Vol. 2 Folds and Fractures*. Academic Press, London.

Rispoli, R. 1981. Stress fields about strike-slip faults inferred from stylolites and tension gashes. *Tectonophysics* **75**, T29–T36.

Segall, P. & Pollard, D. D. 1983. Nucleation and growth of strike-slip faults in granite. *J. geophys. Res.* **88**, 555–568.

Shamina, O. G., Pavlov, A. A., Strizhkov, S. A. & Kopnichev, Yu, F. 1975. Ultrasonic sounding of region of preparation of solitary microcrack. In: *Physics of the Earthquake Focus* (edited by Sadovskii, M. A.). Nauka, Moscow, 92–119. English translation published by Amerind, New Delhi, India (1985).

Sibson, R. H. 1994. Crustal stress, faulting and fluid flow. In: *Geofluids: Origin, Migration and Evolution of Fluids in Sedimentary Basins* (edited by Parnell, J.) *Spec. Publs geol. Soc. Lond.* **78**, 69–84.

Tchalenko, J. S. 1970. Similarities between shear zones of different magnitudes. *Bull. geol. Soc. Am.* **81**, 1625–1640.

Wawersik, W. R. & Brace, W. F. 1971. Post-failure behaviour of a granite and diabase. *Rock Mech.* **3**, 61–85.

Whittaker, A. & Green, G. W. 1983. Geology of the Country Around Weston-super-Mare, memoir for 1:50,000 geological sheet 279 new series, with parts of sheets 263 and 295. Geological Survey of Great Britain, Institute of Geological Sciences, Her Majesty's Stationary Office.

Yoffe, E. H. 1951. The moving crack. *Phil. Mag.* **42**, 739.